RSC Sustainability

ROYAL SOCIETY OF CHEMISTRY

PAPER

View Article Online
View Journal | View Issue

Cite this: *RSC Sustainability*, 2024, **2**, 2693

Synthesis of hydrogels based on sterculia gum-*co*-poly(vinyl pyrrolidone)-*co*-poly(vinyl sulfonic acid) for wound dressing and drug-delivery applications

Ankita Kumari and Baljit Singh *

Much research is currently focused on designing functional materials derived from sterculia gum (SG) for sustainable development. Herein, poly(vinylsulfonic acid) (poly(VSA) and poly(vinyl pyrrolidone) (PVP) was grafted onto SG to form semi-interpenetrating network (semi-IPN) hydrogels for use in a drug-delivery (DD) system for doxycycline and in hydrogel wound dressings (HWDs). The hydrogels were characterized using FESEM, EDS, AFM, FTIR spectroscopy, ^{13}C-NMR, and XRD. A range of biomedical properties were assessed by evaluating the interactions of the hydrogels with blood, mucosal tissues, and drugs. In the FTIR analysis, bands were observed at 1288 and 1149 cm^{-1} due to asymmetric and symmetric stretching of SO_2 of poly(VSA) along, while in the ^{13}C-NMR analysis, a peak at 63.21 ppm was noted due to a carbon attached to a sulfonic acid group of poly(VSA), confirming the polymerization reactions. The hydrogels were found to be biocompatible (hemolysis analysis = 2.54 ± 0.02%) and mucoadhesive (detachment force = 91.0 ± 8.0 mN). The semi-IPN HWDs exhibited antioxidant and antimicrobial properties. The dressings were permeable to oxygen and water vapor but impermeable to microbes. The diffusion mechanism of doxycycline from the dressings was found to follow a non-Fickian mechanism. The release profile could be best described by the Higuchi kinetic model. Overall, these properties revealed that the drug-encapsulating hydrogels could be applied as materials for DD and wound dressing.

Received 30th May 2024
Accepted 24th July 2024

DOI: 10.1039/d4su00273c

rsc.li/rscsus

Sustainability spotlight

Recently, research has predominately centered on designing materials from natural resources to promote sustainable development. These materials find widespread applications in biomedical fields and the creation of healthcare products. Sterculia gum, a natural polysaccharide, has been explored for developing wound dressings and their utilization offers a safer and eco-friendly approach to wound care while aligning with the increasing demand for sustainable and biocompatible materials. This work aligns with the UN's Sustainable Development Goals number 3 and 9. As it is the sustainable renewable product in the form of bioactive hydrogel wound dressings for good health and well-being.

1 Introduction

Recently, much research has focused on designing materials from natural resources to promote sustainable development. These natural polymer-derived materials have widespread applications in biomedical fields and in fabricating various health care products because of their diverse physiological attributes. A plethora of biomaterials have been developed to design wound dressings (WDs) for efficient wound healing.[1] However, the prime focus is to design materials that meet the ideal characteristics of the hydrogel dressing. Hydrogels are porous sponge-like structural analogs, matching the extracellular matrix with a tissue-like consistency, and have been extensively explored for effective wound-healing applications.[2] The impregnation of a therapeutic curing agent in hydrogel wound dressings (HWDs) can further improve their wound healing potential by preventing microbial infection.[3] The modulation of properties of HWDs has been carried out to enhance the efficacy of dressings in diverse wound scenarios.[4] Biopolymer-based HWDs fulfill the essential criteria of a WD by allowing the passage of wound fluid through the dressing material. Bioactivity may be provided to the HWD by incorporating bioactive natural polymers that are therapeutically useful for the healing process.[5]

Sterculia gum (SG) is a bioactive polysaccharide that has been found to be useful in wound healing.[6] Its anti-inflammatory activity reduces swelling of the wound area.[7] Sousa and coworkers[8] reported gastro-protective activities of an ethanol extract of sterculia stem bark in gastric ulcers induced by different agents in mice and rats. Sterculia extract has demonstrated healing properties with antioxidant/antimicrobial activities.[9] SG is a heteroglycan, composed of glucuronic and galacturonic acids along with galactose and rhamnose (partially acetylated). It mainly consists of 55–60% neutral monosaccharide residues, 8% acetyl

Department of Chemistry, Himachal Pradesh University, Shimla-171005, India. E-mail: baljitsinghhpu@yahoo.com

groups, and 37–40% uronic acid residues.[10] It is utilized in making DD formulations for wounds as dressing materials, attributed to its good rheological characteristics.[11] Drápalová and coworkers[12] designed SG-chitosan based dressings that revealed good biocompatibility and a non-cytotoxic nature. Modifications of SG through grafting, thiolation, carboxymethylation, and esterification have led to the design of materials for biomedical uses.[13–15] These modifications improved the physicochemical characteristics of SG and enhanced the chemical/mechanical stabilities. A wide range of modifications in gum-developed materials has led to their increasing utilization in the biomedical sector and pharmaceutical industries.[16]

Poly(vinylsulfonic acid) (poly(VSA)) is a polar water-soluble polymer, wherein charged sulfonate groups provide some useful interactions with biomolecules and also provide blood-compatible features to the hydrogels. Kim and coworkers[17] found that the incorporation of sulfur polymers into the matrix reduces protein adhesion by virtue of its polarity. Lee and coworkers[18] demonstrated that the inclusion of sulfonate is a particularly favorable option for coating materials intended to enhance blood compatibility. Hong and coworkers[19] improved the fluid absorption of a hydrogel by adding poly(VSA) in copolymers. The inclusion of sulfonate functionalities into the backbone led to a reduction in protein/platelet adsorption. PVP is a water-soluble biocompatible additive and film-forming agent used for pharmaceutical medicaments.[20,21] Its addition into pharmaceutical formulation can modify the release profile of a drug.[22] Its blending with polysaccharides improves the swelling of hydrogels.[23] PVP-based polymer matrices have been utilized in DD.[24] Recently, Kuperkar and coworkers[25] provided updated information on natural and synthetic degradable polymers relevant to biomedical applications. Various approaches for the transformation of these polymers by blending, physical/chemical crosslinking, hybrid compositing, and incorporating interpenetrating complexes and *block graft* copolymers have been explored. Poonguzhali and coworkers[26] found an enhancement in the healing rate, re-epithelialization, and wound contraction by applying PVP-chitosan-cellulose dressings. Doxycycline (a tetracycline drug) promotes dermal healing by inhibiting protease activity and reducing inflammation. The impregnation of the antibiotic drug doxycycline in a HWD can facilitate the healing process.[27]

The prime target of the present work was to develop semi-interpenetrating network (semi-IPN) hydrogels for wound dressing and DD utilization. The hydrogels were designed through the grafting reactions of poly(VSA)-PVP polymers onto SG. The antibiotic drug doxycycline was encapsulated within these hydrogels to enhance their wound-healing potential. We also explored the inherent properties of SG, poly(VSA), and PVP for achieving better healing, along with the encapsulation of doxycycline to enhance their healing potential.

2 Experimental

2.1 Materials

SG (MW = 9,500 K, viscosity of 0.5% aqueous solution at 25 °C = 3.38 cP) [Sigma-Aldrich, USA], poly(vinyl pyrrolidone) (PVP)/1-ethenylpyrrolidin-2-one (MW = 40 K, viscosity of 5% aqueous solution at 25 °C = 2.4 cP) [Loba Chemie Pvt Ltd], vinyl sulfonic acid (VSA)/ethenesulfonic acid [Sigma-Aldrich, USA], *N*,*N*′-methylenebisacrylamide (NNMBA)/*N*,*N*′-methylenedi(prop-2-enamide) [Sigma-Aldrich, USA], DPPH (2,2-diphenyl-1-picrylhydrazyl)/2,2-diphenyl-1-(2,4,6-trinitrophenyl)hydrazin-1-yl, FC reagent/1,2-naphthoquinone-4-sulfonic acid sodium salt (Folin–Ciocalteu reagent), doxycycline/(4s, 4aR, 5S, 5aR, 6R, 12aR-4-(dimethylamino)-1,5,10,11,12a-pentahydroxy-6-methyl-3,12-dioxo-4a,5,5a,6-tetrahydro-4*H*-tetracene-2-carboxamide [Nixi Laboratories Pvt Ltd] were the key materials used in the synthesis of the hydrogels. The supplier of the goat-bio-membrane was the Slaughter House (Lal Pani, Shimla, India).

2.2 Synthesis of the network hydrogel dressings

Synthesis of the semi-IPN hydrogels was carried out by grafting reactions of VSA and PVP onto SG. To prepare the hydrogels, hydrated solutions of 5% (w/v) SG and 3% (w/v) PVP were combined with a solution of the monomer [VSA = 4.51×10^{-1} mol L^{-1}], crosslinker [NNMBA = 1.621×10^{-2} mol L^{-1}], initiator [APS = 1.095×10^{-2} mol L^{-1}], and plasticizer [glycerol = 2.56×10^{-1} mol L^{-1}]. Then the mixture was stirred for 3 h at 100 rpm on an overhead stirrer to ensure homogeneity. The reaction mixture was then transferred to Petri plates and placed in an oven set at 65 °C for 2 h under ambient air conditions. PVP and ploy(VSA) grafting was done onto SG in the presence of the crosslinker NNMBA, and hydrogel dressings synthesis was done by a solvent-casting method. Subsequently, washing and drying of the product was done until a constant weight was achieved. The final product was termed as SG-PVP-cl-poly(VSA) semi-IPN hydrogels or dressings. For synthesis of the hydrogels, optimization of reaction parameters was done by varying the monomer VSA from 0.9×10^{-1} to 4.51×10^{-1} mol L^{-1}, while PVP was varied from 1% to 5% (w/v) and NNMBA was changed from 0.324 to 1.621×10^{-2} mol L^{-1} during the polymerization reactions. The optimized reaction parameters were evaluated as SG = 5% (w/v), VSA = 4.51×10^{-1} mol L^{-1}, NNMBA = 1.621×10^{-2} mol L^{-1}, APS = 1.095×10^{-2} mol L^{-1}, and glycerol = 2.56×10^{-1} mol L^{-1} from the swelling data. The optimized HWDs were tested for DD and biomedical analysis.

The crosslinked network structure was developed by grafting poly(VSA) and PVP onto SG in the presence of the crosslinker NNMBA. VSA is a functional monomer and was grafted onto the natural polysaccharide SG and PVP. The covalent linkage developed by monomer grafting formed an insoluble semi-IPN structure, which could retain structural integrity during the *in vitro* DD and biomedical tests. Here PVP is a biocompatible material that also acted as a film-forming agent.

2.3 Characterizations

Field-emission scanning electron microscopy (FESEM)/Energy-dispersive spectroscopy (EDS), atomic force microscopy (AFM), Fourier-transform infrared spectroscopy (FTIR), carbon-13 nuclear magnetic resonance (^{13}C-NMR), and X-ray diffraction (XRD) techniques were applied for characterization of the SG-PVP-cl-poly(VSA) hydrogels. FESEM and EDS were performed

on a SU8010 instrument (Hitachi). AFM was performed on an INTEGRA system (NT-MDT, Russia). FTIR spectra of the dried powdered samples were collected in KBr pellets and recorded on a BRUKER ALPHA Platinum ATR instrument. The solid-state ^{13}C-NMR spectra were obtained on a JEOL ECZR Series 600 MHz NMR spectrometer (Japan). XRD was performed on a PAN-analytical X'pert Pro system (Netherlands).

2.4 Swelling/drug-release properties

Water uptake by the semi-IPN hydrogels was assessed by measuring the weight of the HWD at the start and end of the experiments in various fluids. The swelling was noted in the medium at different pH to simulate/mimic the conditions of bio-fluids or SWF (simulated wound fluid). Drug loading into the hydrogels was done in a 500 μg mL^{-1} solution of doxycycline. The drug-release and -loading experiments were performed in different pH media and data were obtained from the standard curves in buffer solutions of pH 2.2 (λ_{max} = 369 nm), pH 7.4 (λ_{max} = 369 nm), and SWF of pH 8.0 (λ_{max} = 378 nm).[28,29] Drug-calibration curves were prepared using a UV–visible spectrophotometer. The drug-release diffusion mechanism from the drug-loaded hydrogel samples was evaluated using equations given by Ritger–Peppas.[30,31] Release data were analyzed by different kinetic models analyses for obtaining the best fit kinetic models for the release of the drug from the drug-loaded hydrogels.[32]

2.5 Physicochemical and biomedical assay

The SWF uptake by the semi-IPN hydrogels under simulated conditions was analyzed. The increase in weight was noted after keeping the SWF in solution for different time intervals (1 h intervals) at 37 °C. During the blood-compatibility test, the thrombogenicity and hemolysis values were determined after the hydrogel–blood interactions.[33] The thrombogenicity was measured by the weight method and its value was obtained from the clots formed during polymer–blood interactions. Hemolysis was measured from the optical densities (ODs) of the supernatants at 540 nm using a UV–visible spectrophotometer.

The mucoadhesion test was performed by utilizing a goat biomembrane to obtain the detachment force and work of adhesion.[34] DPPH and FC reagent were utilized to obtain the antioxidant characteristics of the hydrogel materials.[35] Winkler's method[36] was applied for determining the O_2 permeability property, while H_2O permeability determined by the desiccant method.[37] Microbial penetration was tested by a turbidity procedure.[38] The porosity of the HWD was obtained from the C_2H_5OH diffusion method.[39] Mechanical attributes, such as the tensile/burst strength (TS/BS), were noted together with the elasticity and resilience/relaxation of the WD.[40] A texture analyzer was used for the adhesion and mechanical tests. The protein-adsorption study was carried out by Lowry's method.[41] Antibacterial testing of the hydrogel with and without a drug was carried out against the bacteria *Staphylococcus aureus* and *Pseudomonas aeruginosa* using the agar well diffusion method along with the pure drug. Agar-spread Petri plates were used for the antibacterial tests.[42]

3 Results and discussion

3.1 Characterizations

3.1.1 FESEM and EDS. FESEM demonstrated there were alterations in the morphological characteristics of polysaccharide gum after modification through grafting/crosslinking reactions (Fig. 1a and b). These images revealed the heterogeneous, irregular, uneven morphology of the semi-IPN matrix. The morphology of the grafted product was different from that of SG, which revealed a flat homogeneous structure in the FESEM images. In the present case, the HWD morphology was found to be somewhat uneven with a random, fibrous network with large irregularly sized pores in the crosslinked HWD. This morphological feature could be useful for fluid sorption and DD. Bashir and coworkers[43] examined the surface morphology a SG hydrogels and found a fibrous microstructure within the hydrogels, characterized by inter-connected pores between the fibers. During the EDS analysis of SG-PVP-poly(VSA) HWDs, peaks due to carbon, oxygen, nitrogen, and sulfur elements were observed in the EDS spectrogram. The elements in the hydrogels included carbon (with a weight percentage of 47.6%), oxygen (42.3%), nitrogen (4.7%), and sulfur (5.5%), indicating the presence of poly(VSA), PVP, and the crosslinker NNMBA. After the formation of the SG-PVP-poly(VSA) HWD, nitrogen and sulfur in the hydrogels indicated the grafting of poly(VSA) and PVP onto SG.

3.1.2 AFM. The AFM image of SG-PVP-poly(VSA) HWD shows the surface topography (Fig. 1c). The root mean square roughness (25.3 nm) and average roughness (18.9 nm) were recorded, which revealed the semi-IPN hydrogels surface obtained through the incorporation of PVP-poly(VSA) into SG by grafting and crosslinking reactions was rough. Roughness provides mucoadhesive attributes to materials and is useful for their site-specific DD. The rough surface of the film can also be helpful for adherence to tissue and favors cellular activity. The incorporation of gum also induced a mucoadhesive character in the DD carrier. Rehmani and coworkers[44] observed a rough surface morphology of a semi-IPN polymeric matrix with ridges and wrinkles/cracks, which were suitable for adhesion of the polymer to the biomembrane.

3.1.3 FTIR. In the FTIR spectra of SG and SG-PVP-poly(VSA) hydrogel (Fig. 2), SG revealed bands at 3360 cm^{-1} [–OH str.], 2914 cm^{-1} [C–H str. of SG], 1716 and 1601 cm^{-1} [C=O str. of carboxylic acid and galacturonic acid ester of SG], 1414 cm^{-1} [–CH_2 bending], and 1033 cm^{-1} [due to C–O–C stretching].[45] The FTIR spectrum of the semi-IPN hydrogels displayed bands at 3390 cm^{-1} [due to –OH groups of SG and poly(VSA)], 2933 cm^{-1} [C–H str. methyl and methylene of SG, poly(VSA) and PVP], 1727 and 1647 cm^{-1} [C=O stretching of carboxylic acid and methylated galacturonic acid ester of SG and C=O str. of PVP], 1424 cm^{-1}[–CH_2 bending of SG, –CH_2 bending of PVP], 1288 cm^{-1} [asymmetric stretch of SO_2 and C–N vibration of PVP], 1149 cm^{-1} [SO_2 symmetric str.], 1033 cm^{-1} [C–O–C stretching of SG and stretching mode of S=O], and 603 cm^{-1} [C–S stretching vibration of poly(VSA)].[46,47] The presence of

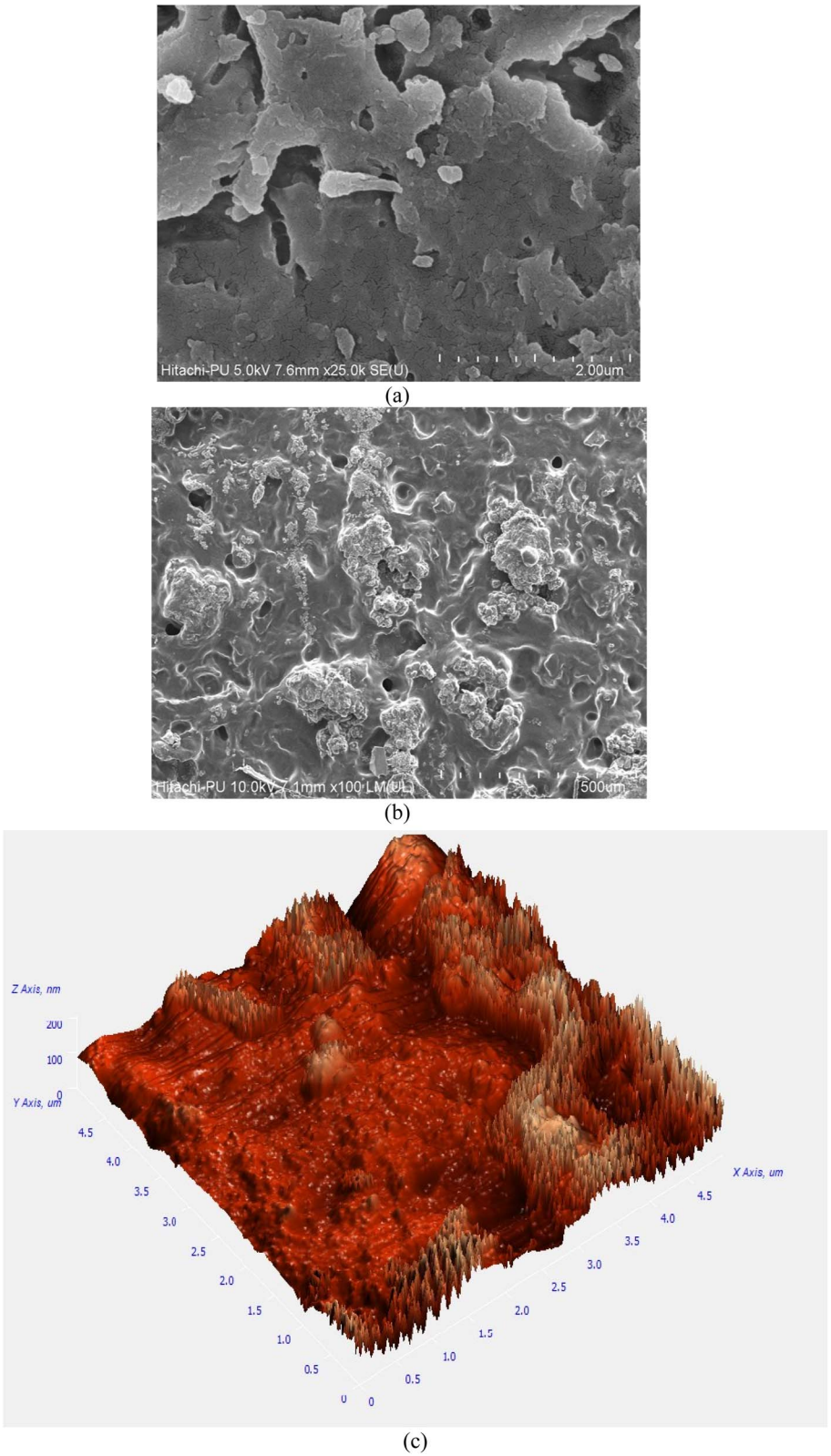

Fig. 1 FESEM images of (a) SG and (b) SG-PVP-poly(VSA) hydrogels; and AFM image of (c) SG-PVP-poly(VSA) hydrogels.

bands at 1288 and 1149 cm^{-1} was due to asymmetric and symmetric stretches of S=O of SO_2 of poly(VSA), which, along with the bands at 1033 cm^{-1} (stretching mode of S–O) and 1647 cm^{-1} (C=O stretching of amide of PVP), confirmed the grafting of poly(VSA) and PVP onto SG during the copolymerization reaction.

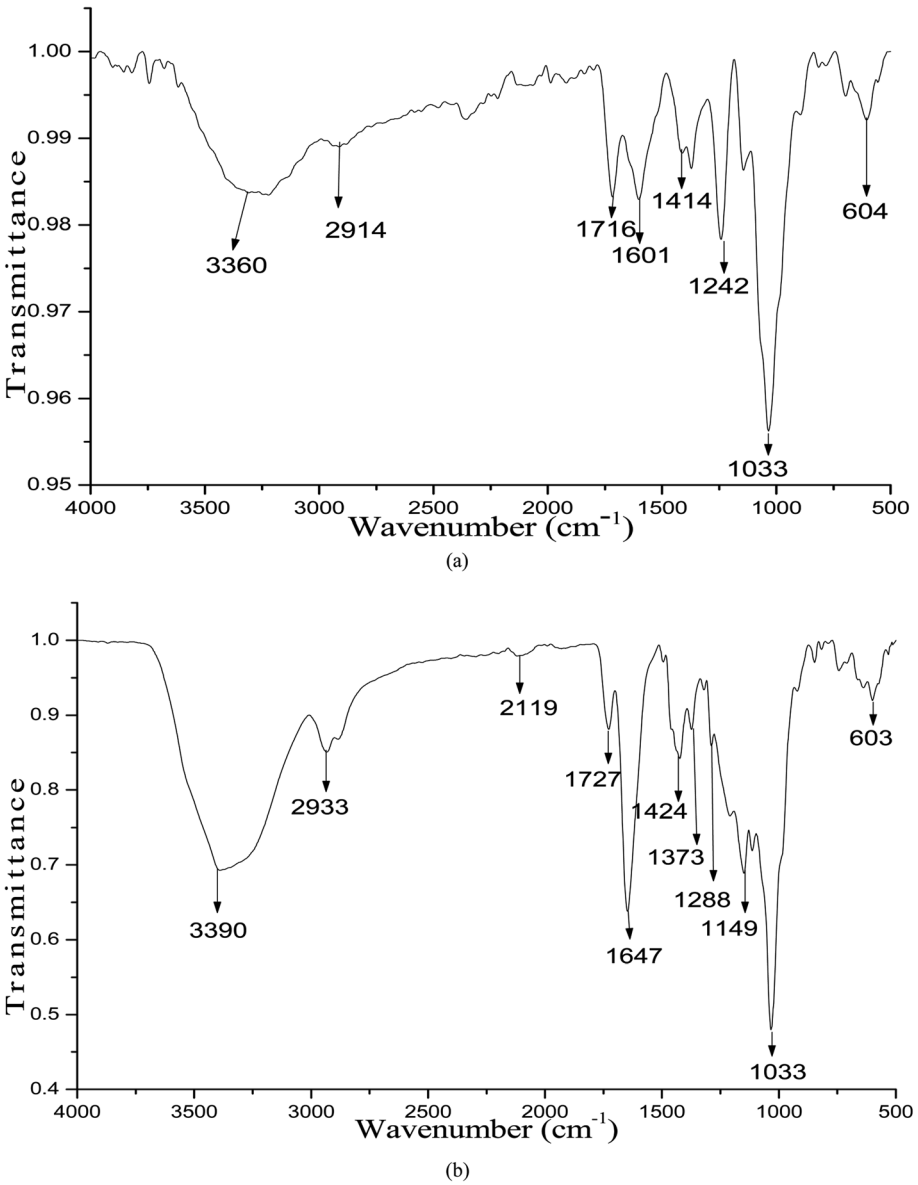

Fig. 2 FTIR spectra of (a) SG and (b) SG-PVP-poly(VSA) hydrogels.

3.1.4 ^{13}C NMR. The ^{13}C NMR spectra of SG and semi-IPN hydrogels [SG-PVP-poly(VSA)] are given in Fig. 3. NMR of SG showed peaks at 173.03 ppm [**C**=O of galacturonic acid of gum], 103.95 ppm [**C**-1 of pyranose rings of SG], around 71.79 ppm [ring carbon **C**-2 to **C**-5 of galacto and glucopyranose ring in gum], 20.69 and 17.10 ppm [CH_3 carbon of rhamnose].[48,49] The ^{13}C NMR of the grafted hydrogel revealed peaks at 177.05 and 173.27 ppm [**C**=O of PVP and **C**=O of galacturonic acid of SG], 104.45 ppm [**C**-1 of galacto-glucopyranose ring of SG], 72.40 ppm [**C**-2 to **C**-5 of a ring of galacto-glucopyranosyl of SG], 63.21 ppm [due to –CH_2–**C**H–SO_3H],[50] 43.29 ppm [due to **C**-2 and **C**-3 of PVP and –CH_2–CH–SO_3H of poly(VSA)], 31.59 ppm [due to **C**-1 and **C**-5 of PVP], and between 20.94–17.59 ppm [due to **C**-4 of PVP and **C**H_3 group of rhamnose of SG].[51] Jin and coworkers[51] reported the ^{13}C NMR of PVP and observed peaks at 44 ppm [due to **C**-2 carbon of PVP moiety], 42.5 ppm [due to **C**-3 carbon of PVP moiety], 31.5 ppm [due to **C**-5 carbon of PVP moiety], and 17.5 ppm [due to **C**-1, 4 carbon of PVP moiety]. The inclusion of poly(VSA)-PVP into the hydrogels was confirmed by the appearance of peaks at 177.05 ppm for the carbonyl group of PVP present in the polymers, 63.21 ppm for carbon attached to a sulfonic acid group of poly(VSA), and 43.29 ppm for the **C**-2 and **C**-3 of PVP and –**C**H_2-CH-SO_3H of poly(VSA).

3.1.5 XRD. The XRD spectra of SG and SG-PVP-poly(VSA) HWD are given in Fig. 4. The diffractogram of the gum showed no evident sharp peaks in the diffraction pattern. XRD of SG did not elucidate long-range order and depicted an amorphous state of SG.[52,53] The XRD spectra of SG-PVP-poly(VSA) HWD showed sharp peaks (at 2θ equal to 12.4°, 21.2°) for the modification of SG. The grafting of poly(VSA) onto SG polysaccharide revealed a modification in the crystallinity of the grafted gum. Bahulkar and coworkers[14] studied the X-ray

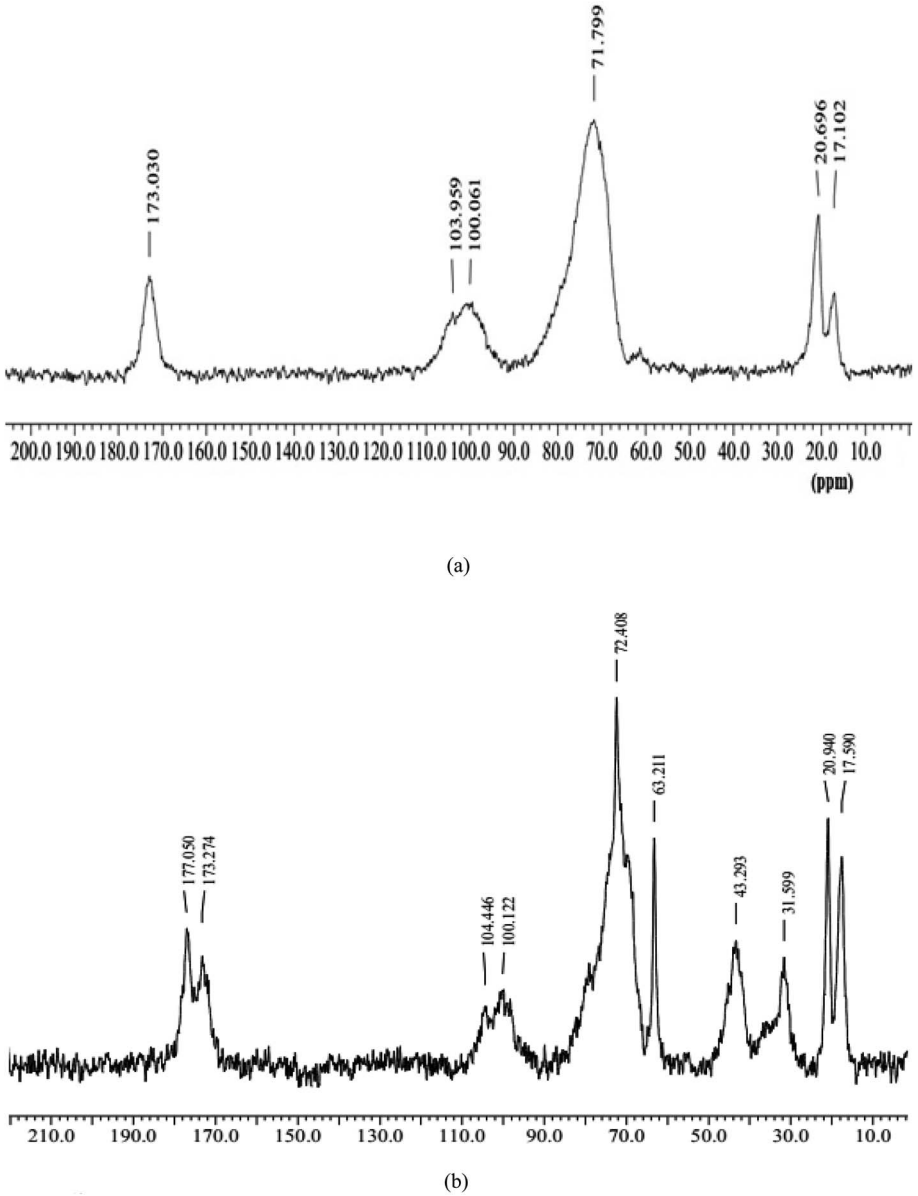

Fig. 3 ^{13}C-NMR of (a) SG and (b) SG-PVP-poly(VSA) hydrogels.

diffractogram of gum, which did not show any sharp peaks, indicating the amorphous nature of karaya gum, while the diffractogram of thiolated gum showed peaks at 22° and 27° with a slightly higher intensity, indicating a change in the crystallinity of the compound.

3.2 Swelling properties

During synthesis, the effect of varying the contents of [VSA], [PVP], and [NNMBA] on the crosslinking of semi-IPN was evaluated by determining their swelling (Fig. 5 and Table 1). A rise in swelling was found in the hydrogels prepared with the increase in [VSA] from 0.5×10^{-1} to 2.66×10^{-1} mol L^{-1} during the copolymerization reactions. The increase in the notable hydrophilic character of HWD was due to the incorporation of more poly(VSA) after the grafting/crosslinking reactions. This amplification in hydrophilicity arose due to the progressive incorporation of poly(VSA) during the crosslinking reactions linked with the more sulfonic acid groups (–SO_3H), which led to a greater affinity for water. Kim and coworkers[17] also revealed the higher swelling of polyacrylic acid-poly(VSA) hydrogels because of the hydrophilicity of the semi-IPN hydrogels. The swelling of HWD first increased with the increase in PVP content from 1% to 3% and subsequently decreased. This could be attributed to the reason that initially, the formation of loose semi-IPN hydrogels occurred, but after optimization of the network formation, the network density started increasing with the rise in [PVP], which gradually diminished the swelling of the hydrogels. Rasool and coworkers[54] established a correlation between hydrogel swelling and time. The diffusion of water into the semi-IPN was responsible for relaxation of the chains during water uptake with increasing the time of swelling.

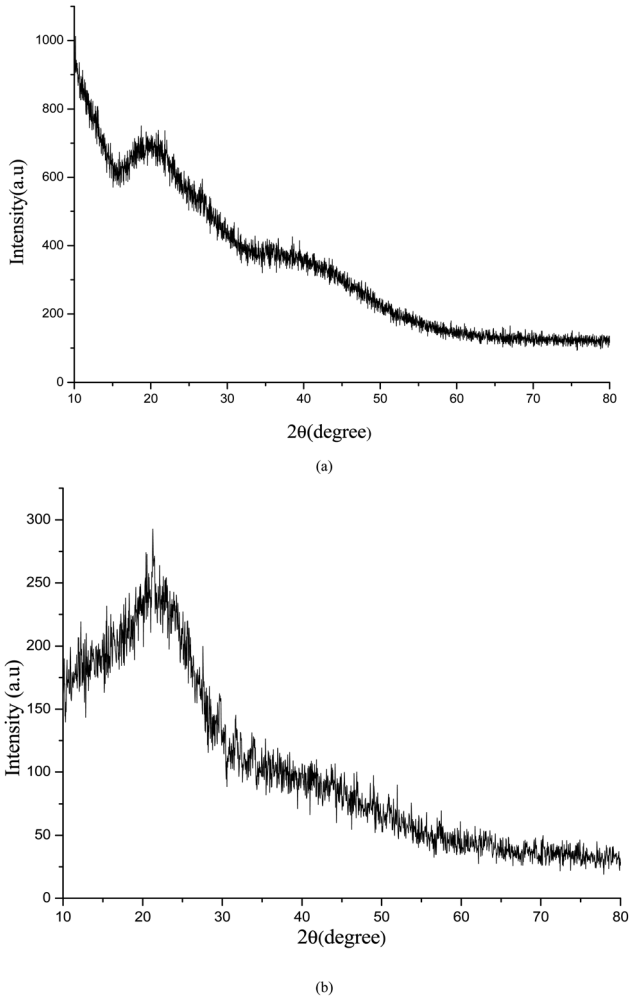

Fig. 4 XRD spectra of (a) SG and (b) SG-PVP-poly(VSA) hydrogels.

The swelling of the hydrogels was reduced with the rise in NNMBA content from 0.324×10^{-2} to 1.62×10^{-2} mol L^{-1} during the synthesis of the hydrogels. These swelling trends could be due to an enhancement in the crosslinking density and reduction in pore size between the network chains of the hydrogel films. Consequently, this led to slow H_2O diffusion into the semi-IPN, thereby restricting chain relaxation and reducing the swelling of the hydrogels. Jalababu and coworkers[55] demonstrated that, as the concentration of NNMBA increased the crosslinking points in the polymeric chains, consequently, less swelling occurred in the hydrogels.

The swelling of the hydrogels in solutions at different pH helped elucidate the effect of the pH of the swelling medium on the solvent-uptake capacity of the hydrogels. More swelling of the HWD in a higher pH medium was observed than that of the other swelling media. This observation may be explained on account of the ionic repulsions among ions formed after partial hydrolysis within the polymers, which led to the expansion of the networks in the higher pH medium. Ionizable carboxylic groups in the gum and sulfonic acid groups of poly(VSA) under basic pH conditions get converted to ($-COO^-$, SO_3^-) and their electrostatic repulsions opened the network of the hydrogels and increased the swelling of the gel. In another research report, poly(acrylic acid)-poly(VSA) hydrogels demonstrated an increase in the swelling ratio with the increase in the pH of the swelling medium, probably due to ionization of the –COOH and $-SO_3H$ groups leading to more hydrogel expansion in the basic solution.[56]

3.3 Drug-release properties

The *in vitro* release dynamics of doxycycline from the drug-encapsulated semi-IPN hydrogels were evaluated in various releasing media, including pH 2.2 buffer, pH 7.4 buffer and SWF at 37 °C (Fig. 5e and Tables 2 and 3). The results of the release profile revealed that the release was more in SWF compared to the other media from the drug-impregnated hydrogels. The drug-release trends from the HWDs were found to run parallel to the swelling trends of the hydrogels. This inferred the pH-responsive release behavior of the hydrogels. Release of the antibiotic drug occurred in a sustained manner without a burst effect and the values of the diffusion coefficients were found to be lower in the later stages. The total monomer concentration of 4.51×10^{-1} mol L^{-1} was found to be suitable for developing network hydrogels as DD carriers with sufficient crosslinking and strength properties. However, the release profile could be tuned by altering the network density by varying the reaction parameters. It has been evidenced in other research that increasing the crosslinking increases the rigidity of the network, also decreasing drug diffusion, and the hydrogel blends found could be fitted for prolonged DD use.[57]

From the preliminary analysis of the swelling/drug-release properties of HWDs in SWF, it could be concluded that these materials have the potential to act as HWDs. The diffusion of doxycycline occurred by a non-Fickian mechanism, which was confirmed from the values of the diffusion exponent '*n*'. The regression coefficient (R^2) values demonstrated that drug release from the hydrogel could be best described by the Higuchi kinetic model. The drug release was slow and occurred in a sustained manner from the hydrogels. Generally, drug release from the matrix is considered as characteristic of the polymer network composition and solubility of the drug. Das and coworkers[58] observed a higher rate of drug was released in a higher pH medium. It has also been illustrated that the release of water-soluble drugs from hydrogels occurs after water penetration into the semi-IPN, subsequently swelling the hydrogels/drug dissolution and releasing the drug from polymer matrix by drug diffusion. In some cases, swelling medium penetration into the network hydrogel, polymer chain relaxation, the formation of a loose structure, and erosion of the polymer matrix control the release of drugs from hydrogels. A graphical representation of the encapsulated drug doxycycline in the hydrogel is shown in Scheme 1.

3.4 Wound-fluid sorption

It was revealed from the results of the fluid absorption test for the semi-IPN hydrogel that these hydrogels could retain a significant content of wound fluid, whereby 1 g of hydrogel dressing absorbed about 6 g of SWF (Table 4). Wound-fluid

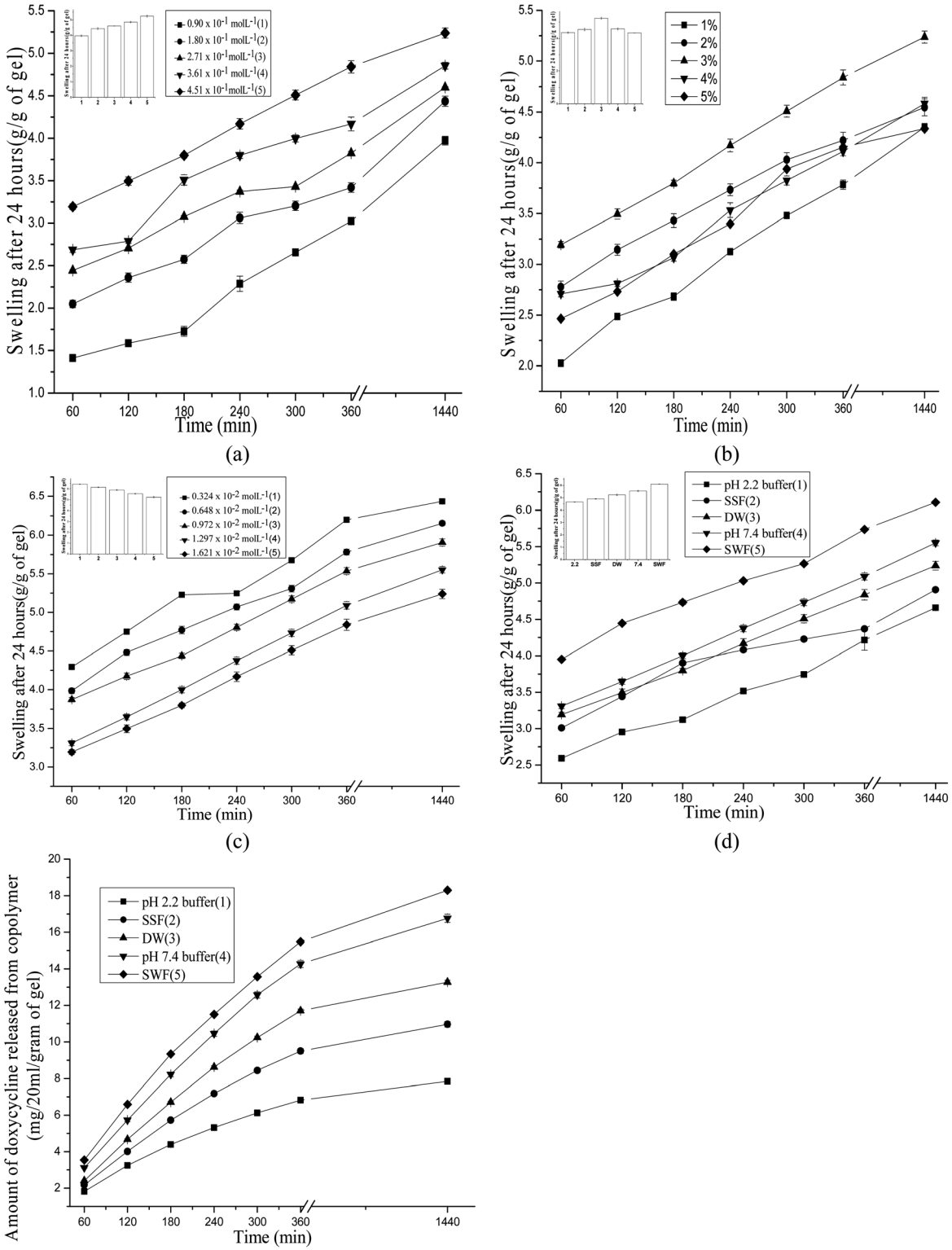

Fig. 5 Effect of (a) [VSA] (b) [PVP] (c) [NN MBA] (d) [pH] on swelling of the hydrogels and (e) release profile of doxycycline from the SG-PVP-poly(VSA) hydrogels.

absorption by the HWDs was because of their network structure and the presence of hydrophilic polar functionalities in the polymer chains present in the hydrogels. Since the pH of artificial wound fluid was 8.0, this led to the ionization of the functional moieties into ions ($-COO^-$, SO_3^-). The ionic pendant groups incorporated into the polymeric chains play a crucial

Table 1 Results of the swelling, diffusion exponent 'n', gel characteristic constant 'k', and various diffusion coefficients for the swelling kinetics of SG-PVP-poly(VSA) hydrogels

S. No.	Parameters	Swelling after 24 h (g g^{-1} of gel)	Diffusion exponent 'n'	Gel characteristic constant 'k' $\times 10^1$	Diffusion coefficients (cm^2 min^{-1})		
					Initial $D_i \times 10^6$	Average $D_A \times 10^6$	Late time $D_L \times 10^6$
Effect of [VSA] $\times 10^1$ (mol L^{-1})							
1	0.9	3.97 ± 0.05	0.43	0.50	1.55	3.42	6.10
2	1.8	4.43 ± 0.06	0.29	1.34	2.86	4.95	5.31
3	2.7	4.59 ± 0.09	0.25	1.89	2.37	7.09	5.79
4	3.6	4.85 ± 0.04	0.27	1.74	3.18	8.34	7.50
5	4.5	5.23 ± 0.06	0.23	2.27	2.76	12.13	9.47
Effect of PVP% (w/v)							
6	1	4.31 ± 0.03	0.34	1.10	4.51	4.07	8.19
7	2	4.56 ± 0.08	0.23	2.27	2.91	7.13	10.1
8	3	5.23 ± 0.06	0.23	2.27	2.76	12.13	9.47
9	4	4.58 ± 0.06	0.24	2.05	2.88	5.77	8.2
10	5	4.33 ± 0.00	0.29	1.58	4.66	5.35	14.0
Effect of [NN-MBA] $\times 10^2$ (mol L^{-1})							
11	0.32	6.43 ± 0.01	0.18	3.02	2.04	5.49	11.3
12	0.64	6.15 ± 0.02	0.19	2.87	2.11	5.08	9.83
13	0.97	5.90 ± 0.04	0.19	2.84	2.16	4.77	9.47
14	1.29	5.52 ± 0.04	0.23	2.15	2.77	4.06	8.87
15	1.621	5.23 ± 0.06	0.23	2.27	2.76	12.13	9.47
Effect of medium of swelling							
16	pH 2.2 buffer	4.66 ± 0.02	0.25	1.87	3.00	3.80	8.32
17	SSF	4.90 ± 0.02	0.21	2.56	2.21	5.42	7.63
18	DW	5.23 ± 0.06	0.23	2.27	2.76	12.13	9.47
19	pH 7.4 buffer	5.55 ± 0.15	0.23	2.15	2.78	4.40	8.87
20	SWF	6.11 ± 0.01	0.19	2.86	2.08	5.88	9.47

Table 2 Results of the diffusion exponent 'n', gel characteristic constant 'k', various diffusion coefficients, and kinetic parameters for the drug-release profile of doxycycline from the drug-loaded SG-PVP-poly(VSA) hydrogels

Release medium	Diffusion exponent 'n'	Gel characteristic constant '$k \times 10^2$'	Maximum amount of released drug, C_{max} (mg L^{-1})	Constant of the kinetic of release $k_{rel} \times 10^6$ (s^{-n})	Initial release rate r_o (mg L^{-1} s^{-1})	Diffusion coefficients (cm^2 min^{-1})		
						Initial $(D_i) \times 10^6$	Average $(D_A) \times 10^6$	Late time $(D_L) \times 10^6$
pH 2.2 buffer	0.74	1.17	233.64	9.85	0.54	11.2	5.9	10.3
SSF	0.83	0.68	460.82	2.86	0.61	13.6	5.6	11.3
DW	0.89	0.49	793.65	1.05	0.66	14.4	5.3	11.8
pH 7.4 buffer	0.86	0.56	813.00	1.27	0.85	12.5	4.9	10.0
SWF	0.82	0.68	729.92	1.86	0.99	11.8	4.8	9.65

role in inducing ionic repulsion, leading to an expansion of the network within the hydrogels and simultaneously an enlargement of the pores. Additionally, ionization induces (i) polarity, (ii) hydrophilicity, and (iii) consequently more fluid sorption, which can help maintain moist conditions desirable for better healing. This implies that the dressing can retain fluid, which is a critical prerequisite for dressing materials. Hence these HWDs could be applied in handling the wound-fluid content in healing and would be useful for absorption, retention, gelling and moisture transmission.[59] Wound-exudate absorption may assist healing processes by preventing the wound from drying out, while also enhancing the repairing cell migration and providing useful nutrients for cell metabolism.[60]

3.5 Blood compatibility

The results of the interactions of the semi-IPN hydrogels with blood revealed thrombogenicity and hemolysis caused by hydrogels. Thrombogenicity was found to be 86.11 ± 3.47% during the blood clotting test performed with the HWDs (10 × 10 mm) (Table 4). This indicated the non-thrombogenic behavior of the hydrogels. The hemolytic parameter of the semi-IPN was determined to be 2.54 ± 0.02% and so it is considered as non-hemolytic, and safe for biomedical uses. The present copolymeric material illustrated compatibility with blood and fitness for dressing utilization. The hydrophilicity and polarity of the material containing SG, PVP, and poly(VSA)

Table 3 Results of the correlation coefficients (R^2) of different drug-release models for assessing the release profile of doxycycline from the drug-loaded SG-PVP-poly(VSA) hydrogels

		Drug release mediums				
Kinetic model		pH 2.2 buffer	SSF	DW	pH 7.4 buffer	SWF
Zero order	R^2	0.977	0.987	0.992	0.994	0.989
	$K_o \times 10^3$ (min^{-1})	2.1	2.2	2.3	2.2	2.2
First order	R^2	0.980	0.971	0.952	0.964	0.971
	$K_1 \times 10^3$ (min^{-1})	5.8	5.9	6.3	5.6	5.4
Higuchi	R^2	0.999	0.998	0.996	0.995	0.998
	$K_H \times 10^2$ ($min^{-1/2}$)	5.7	6.0	6.3	6.0	5.8
Korsmeyer–Peppas	R^2	0.994	0.997	0.997	0.999	0.997
	$K_{KP} \times 10^1$ (min^{-n})	7.3	8.3	8.9	8.6	8.2
Hixson–Crowell	R^2	0.998	0.995	0.987	0.991	0.994
	$K_{HC} \times 10^3$ ($min^{-1/3}$)	1.3	1.4	1.5	1.3	1.3

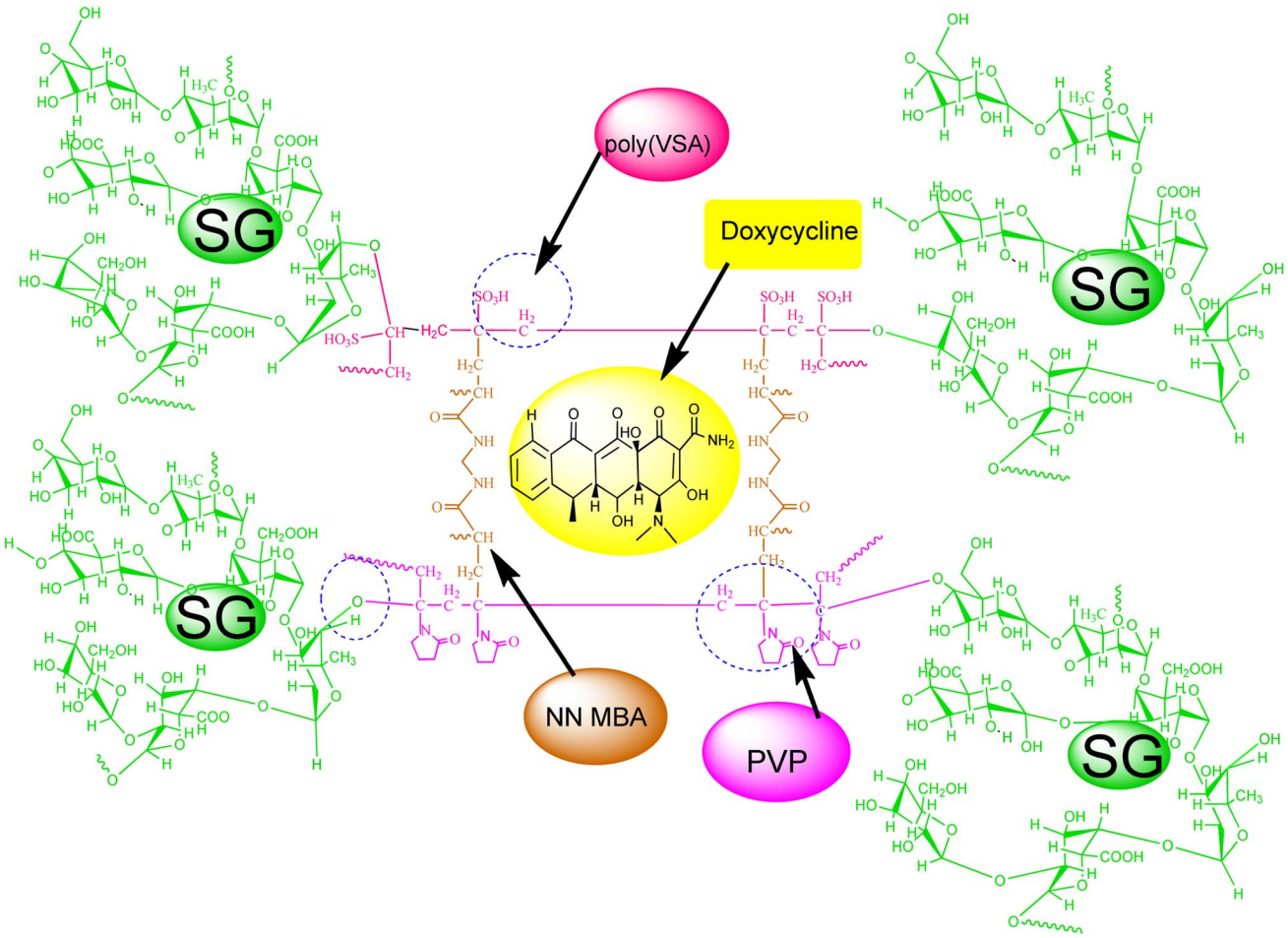

Scheme 1 Graphical representation of the encapsulated drug doxycycline in the hydrogel.

polymers, which comprise various polar functional moieties, including carboxylic group (–COOH), hydroxyl groups (–OH), –N–C=O, sulfonic acid (–SO_3H) groups, respectively, was responsible for the blood-compatibility features of the hydrogels. Due to the hydrophilicity of the HWD decreasing the adherence of semi-IPN hydrogel films with RBCs, there was less disruption to RBCs.

All these contents directly or indirectly contributed to the blood compatibility of the HWDs. PVP and its composite materials are biocompatible. Higuchi and coworkers[61] explained the biocompatible behavior of PVP-modified polysulfone membrane due to the presence of a long hydrophilic side chain of PVP on the membrane. The poly(VSA)-based semi-IPN hydrogels displayed superior biomedical properties, in part

Table 4 Results of the biomedical and mechanical properties of the SG-PVP-poly(VSA) hydrogels

Properties		Inference
Simulated wound-fluid absorption		
6.11 ± 0.01 (g g^{-1} of gel)		
Blood compatibility		
Thrombose percentage (%)	86.11 ± 3.47%	Non-thrombogenic
Hemolytic index (%)	2.54 ± 0.02%	Non-hemolytic
Antioxidant activity		
DPPH assay	Scavenging = 43.813 ± 0.286%	Antioxidant
F–C reagent assay	Gallic acid equivalent = 14.53 ± 0.87 μg	
Mucoadhesion		
Detachment force F_{max} = 91 ± 8.00 mN		Mucoadhesive
Work of adhesion W_{ad} = 0.087 ± 0.001 N mm		
Debonding distance = 3.58 ± 0.255 mm		
Oxygen permeability		
Oxygen present in flask covered with film = 5.33 ± 0.57 mg L^{-1}		Permeable
Water vapor permeability		
Rate of water vapor penetration = 870.30 ± 30.65 g m^{-2} day^{-1}		Permeable
Microbial penetration		
Times (in days, positive control)	Times (in days, negative control and hydrogel dressings)	Impermeable to microbes
30 days = complete turbidity	30 days = no turbidity	
Porosity		
Porosity = 40.225 ± 1.24%		Porous in nature
Mechanical properties		
Burst strength	Bursting strength = 6.65 ± 0.08 N	Mechanically stable
	Distance at burst = 6.51 ± 0.32 mm	
Tensile strength	Tensile strength = 0.117 ± 0.004 N mm^{-2}	
Resilience	Resilience = 88.65 ± 8.27%	
Relaxation	Force at target distance = 0.29 ± 0.03 N	
	Relaxed force = 0.12 ± 0.02 N	
	Retained force = 41.17 ± 0.77%	
Folding endurance	More than 450 times	

related to their negatively charged functionalities, which reduced protein adsorption or platelet adhesion.[62] Generally, protein-adsorption processes lead to platelet adhesion and the activation of coagulation pathways, leading to thrombus formation. Lee and coworkers[18] illustrated that interfacial interactions between the polymer–plasma proteins/platelets are useful for establishing blood compatibility. They reported that the incorporation of sulfonate or sulfonated polyethylene oxide into substrates reduces protein adsorption or platelet adhesion owing to its negative charge character in an aqueous solution. A graphical representation of the repulsive forces among polymer–blood protein during a blood-compatibility test is pictured in Scheme 2.

3.6 Mucoadhesion

The adhesion test of the semi-IPN HWD with a biosurface revealed that a force of 91 ± 8.00 mN was required for separation of the film from goat membrane during the test, which indicated a work of adhesion of 0.087 ± 0.002 N mm for a deboning distance of 3.586 ± 0.25 mm (Table 4). Polymeric HWDs were kept in membrane contact for 60 s with a 0.1 N force before the test experiment. The adhesion test revealed that the HWDs exhibited mucoadhesive properties because of the presence of SG, PVP, and poly(VSA) in the hydrogels, which facilitated non-covalent interactions/hydrophilic forces among the hydrogel–biomembrane. Hydrophilicity to the dressings was provided by the –COOH, –OH, –N–C═O, and $–SO_3H$ functional groups. Prüfert and coworkers[63] found that the mucoadhesive strength of semi-IPN hydrogels containing methylpropane sulfonic acid was due to functionalities present in the hydrogels.

3.7 Antioxidant activity

The semi-IPN HWD exhibited antioxidant properties during the DPPH and FC reagent assay (Table 4). The DPPH assay of hydrogel revealed 38.26 ± 0.51% DPPH active radical trapping/scavenging after 24 h, while the FC reagent displayed an antioxidant activity of 14.53 ± 0.87 μg/100 mg of GAE. Gum sterculia

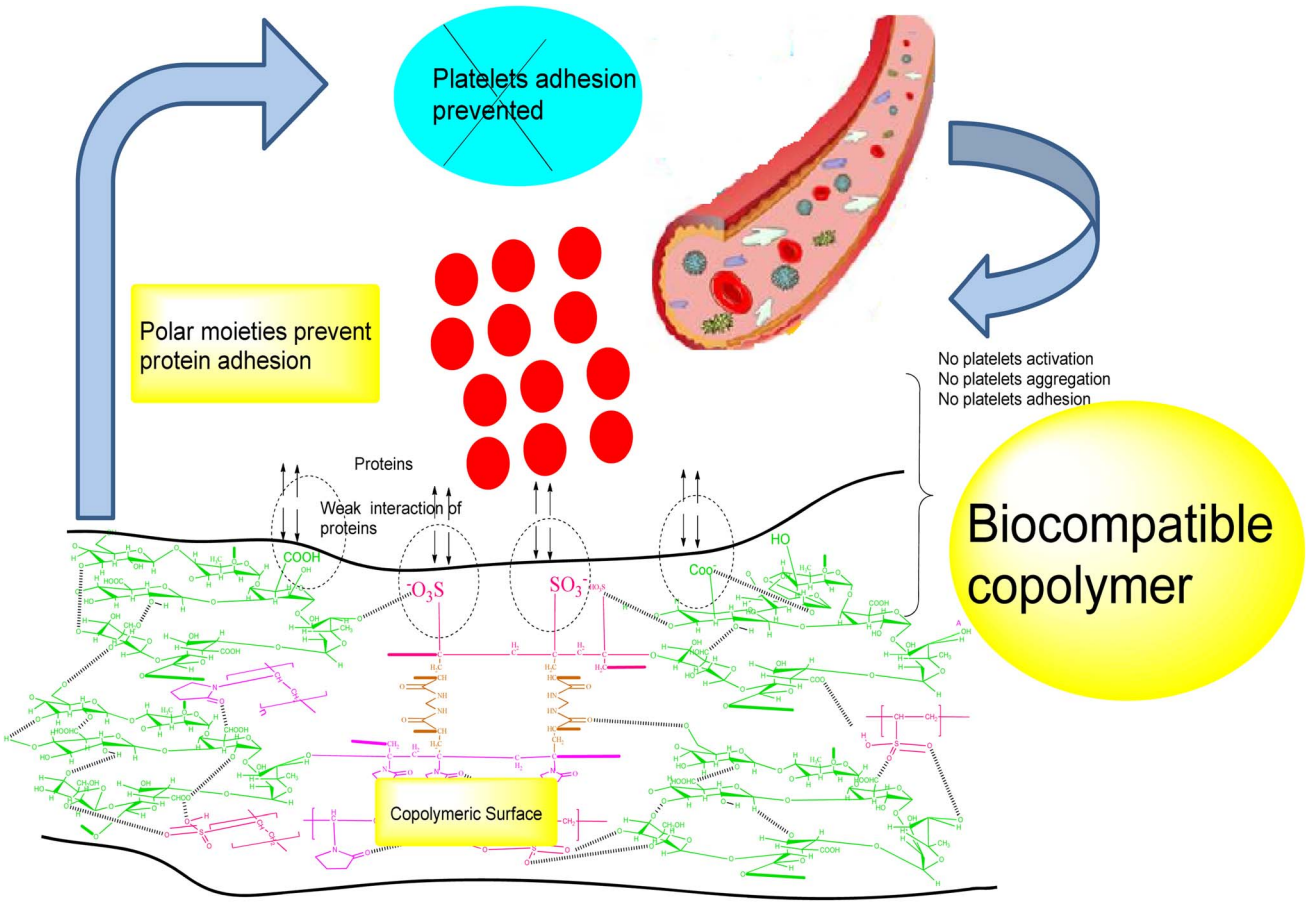

Scheme 2 Graphical representation of the repulsive forces between the polymer–blood protein during the blood-compatibility test.

displayed potential antioxidant features and its presence in the hydrogels may endow them with antioxidant properties that could improve the healing processes. SG has been reported to be a potential antioxidant material that can enhance wound-healing processes.[64] The antioxidant activity of the hydrogels was due to the presence of SG because of its polyphenolics.[65] It has been revealed in various other research reports that the rate of wound healing can be enhanced by the addition of antioxidant compounds.[66] Antioxidants substances counteract the damaging/harmful effects of oxidation in various tissues and can significantly decrease the adverse impact of reactive or oxygen species on physiological functions in humans.

3.8 Oxygen permeability

The O_2 permeability of the semi-IPN hydrogel film was evaluated from the content of dissolved oxygen present in the test experiment for a sample covered with the hydrogel dressing. The hydrogel revealed an O_2 permeability of 5.33 ± 0.57 mg L^{-1} during the experimental observation, and so the HWD exhibited a permeable nature to oxygen diffusion (Table 4). The presence of oxygen is required for a better healing of wounds. The polymeric HWDs were shown to be permeable to oxygen and can provide enough O_2 supply to the wound site for helping tissue/wound maintenance. Some optimized content of the O_2 supply to the wound enhances wound repair and is involved in most significant cellular processes: (i) oxidative phosphorylation in mitochondria leading to ATP production, (ii) oxygen homeostasis, necessary to produce/maintain ATP levels in cells, and (iii) providing energy critical for proper cellular function/protein synthesis.[67]

3.9 H_2O permeability

Water vapor permeability (WVP) tests of the hydrogel were performed with vials covered with SG-PVP-poly (VSA) films, which showed 870.30 ± 30.65 g m^{-2} day^{-1} water permeability, while the value for the open vial was 4419.28 ± 14.34 g m^{-2} day^{-1} (Table 4). The WVP of the polymeric films was thus significantly less than that of the open vials. The hydrogel dressings were permeable to water vapor due to the porous nature of the network HWD. It revealed that these hydrogel dressings could efficiently prevent excessive dehydration from the wound site, an ideal characteristic of HWD materials. Optimized HWD materials make it possible to create a balanced environment that can prevent both dehydration and the accumulation of excess H_2O vapor. Total dehydration of the wound surface will occur in cases where there is a high WVP, while maceration of the surrounding tissues of the wound will occur with a low WVP in dressing, which can be painful during

detachment of the dressing. The permeability characteristics of the hydrogels to water vapor are advantageous compared to conventional dressings for wounds.[68] Barros and coworkers[69] found that the presence of alginate in alginate-rubber latex membranes increased the WV permeability compared to pure natural rubber latex.

3.10 Microbial penetration

Microbial penetration of the hydrogel dressing revealed the impermeable nature of the dressing to microorganisms (Table 4). This may be due to the crosslinking present in the hydrogels, which inhibited microbial penetration. This can reduce the chances of secondary infection during healing. Zheng and coworkers[70] performed microbial penetration tests on PVP-based HWDs, and the microbe penetration tests revealed their impermeable nature and reduced bacterial contamination of wounds. Overall, it was revealed that no bacteria penetrated through the hydrogel samples.

3.11 Porosity

The hydrogel exhibited 40.22 ± 1.24% porosity in the semi-IPN (Table 4). The formation of a network structure during the crosslinking reaction was the reason for the porous nature of the hydrogel dressings. This is thus a useful characteristic dressing material for the sorption of wound fluid, which can provide moisture for better wound healing. The porosity of the

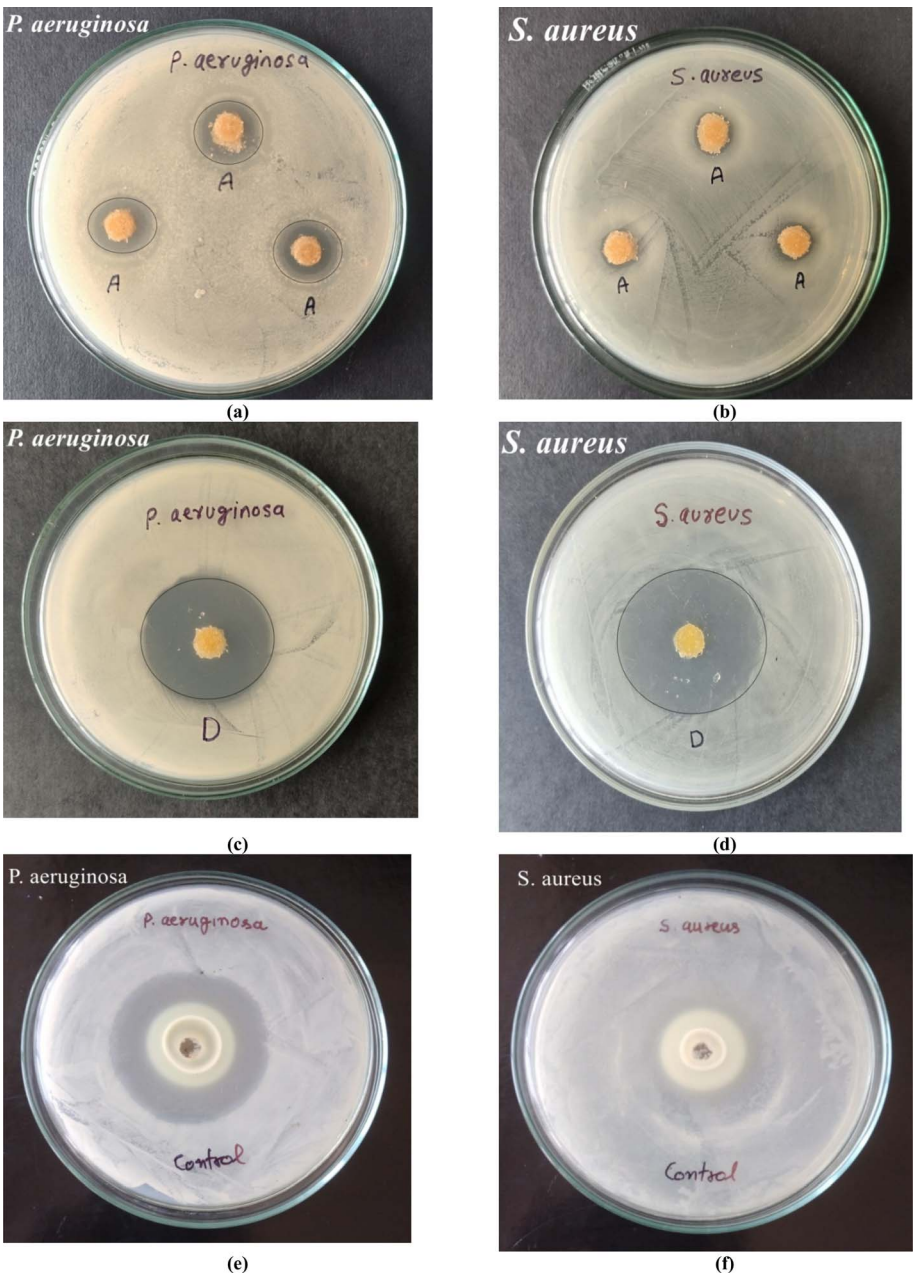

Fig. 6 Antibacterial activity of (a and b) hydrogels, (c and d) drug-loaded hydrogels, and (e and f) drug doxycycline against *P. aeruginosa* and *S. aureus* bacteria.

hydrogels also provided permeability to O_2 and WV through the dressings. The addition of NNMBA was a contributing factor in controlling the crosslinking in the HWD. The porous morphology of karaya gum-chitosan hydrogels facilitated their effectiveness for wound-fluid absorption.[12] A karaya gum-acrylate-grafted hydrogel illustrated an irregular and porous structure. The permeable structure of the hydrogel may also facilitate the exchange of other gasses during wound healing.[71]

3.12 Antimicrobial activity

The antimicrobial activity of the hydrogels (with and without drug) and the pure drug is illustrated in Fig. 6. Both Gram-positive bacteria (*S. aureus*) and Gram-negative bacteria (*P. aeruginosa*) were chosen for evaluating the antibacterial activities of the hydrogels. The hydrogel dressing revealed bactericidal activity against these bacteria and the results demonstrated an average inhibition zone of 5.66 ± 0.57 mm against *P. aeruginosa*, while it was 2.8 ± 0.28 mm for *S. aureus*. The doxycycline-encapsulated polymer dressings inhibited the bacteria growth and showed inhibition zones of 33 mm and 34 mm against the bacteria *P. aeruginosa* and *S. aureus*, respectively. The pure drug was also subjected to antimicrobial evaluation and inhibition zones of 37 mm and 33 mm were observed against the bacteria *P. aeruginosa* and *S. aureus*, respectively. Jhonson and coworkers[72] evaluated the antimicrobial property of doxycycline-loaded hydrogels against four periodontal pathogens and found that the drug-loaded hydrogels possessed greater antimicrobial activity, which was also drug concentration-dependent.

3.13 Mechanical properties

The mechanical strength in terms of the TS and BS of dressings along with resilience/stress relaxation and folding endurance are given in Table 4. TS was recorded as 0.12 ± 0.004 N mm^{-2} and the BS of the materials was found to be 6.65 ± 0.08 N at a burst distance of 6.51 ± 0.32 mm. The films revealed a 0.29 ± 0.03 N stress relaxation force and 41.17 ± 0.77% relaxation during the relaxation tests of the films (0.134 ± 0.002 cm). The resilience test showed 88.65 ± 8.2% resilience with a 0.382 ± 0.47 N force at the target distance. The HWDs depicted viscoelastic behavior in the polymer film. The hydrogel dressings remained intact during the folding endurance test, even after folding/de-folding more than 450 times, reflecting the mechanical elasticity in the films, which would be suited for joint injuries wound dressings. The TS and BS of HWD were because of the covalent linkages during crosslinking in the hydrogel films together with some physical interactions among the various components in the HD. Covalent bonding formed by poly(VSA) and PVP grafting onto the gum along with the crosslinker improved the mechanical strength. Some degree of strength is needed in a material to be applied for dressing purposes to joints in a biosystem along with elasticity properties. The addition of glycerol in the film provided elasticity to the polymeric films. In one study, poly(acrylic acid)-poly(VSA)-based hydrogels were employed as an artificial muscle because these hydrogels showed a contraction and expansion behavior similar to a natural muscle.[17] The SG-based HWD has the desired mechanical properties. The results demonstrated the strength of the hydrogel dressings together with the elasticity needed for wound protection; hence these films were not found to be prone to rupture and could be applied for skin injuries.

3.14 Protein adsorption

Protein-adsorption tests with the SG-PVP-poly(VSA) hydrogels showed that the films had 7.0 ± 1.41% albumin adsorption during the test performed for 24 h at 37 °C. This shows the hydrophilic and hydrophobic balance of the constituent chains present on the polymer surfaces, which controls the protein-adsorption property of the hydrogels and subsequent platelet adhesion to polymer surfaces. Other research reports have confirmed that, in general, a hydrophobic surface tends to attract more proteins than a hydrophilic surface.[73] Since the SG-PVP-poly(VSA) hydrogels were hydrophilic, this led to a reduction in protein adsorption. It also contributed to the biocompatibility of the hydrogels. However, albumin deposition can be minimized if the material exhibits a net negative charge and relatively more hydrophilic features.[74]

4 Conclusions

In summary, crosslinking of the SG-PVP-poly(VSA) hydrogels was controlled by changes in the VSA, PVP, and NNMBA content feed during synthesis, as evident from the results for the swelling properties. The hydrogels demonstrated a good SWF absorption ability, which is useful to maintain moist wound surroundings conducive to healing. An uneven morphology and rough surface were illustrated by the FESEM and AFM analyses. Further, the inclusion of poly(VSA), PVP onto the gum was evident from the ^{13}C-NMR and FTIR analyses. The dressing illustrated biocompatible (hemolysis analysis = 2.54 ± 0.02%) and mucoadhesive (detachment force = 91.0 ± 8.00 mN) properties. The semi-IPN hydrogels exhibited antioxidant and antimicrobial characteristics. The dressings were permeable to O_2/H_2O but impermeable to microbes. The diffusion mechanism of doxycycline from the dressings was non-Fickian and the release could be best explained by the Higuchi kinetic model. Drug release was slow and occurred in a sustained manner. Overall, these properties revealed that the doxycycline-encapsulated semi-IPN could be applied as a material for wound dressing and DD utilization.

Data availability

All the data supporting this article have been included in the manuscript in the form of tables/figures and no other research results, software or code are available.

Conflicts of interest

There are no conflicts of interest to declare.

References

1 Y. Liang, J. He and B. Guo, *ACS Nano*, 2021, **15**(8), 12687–12722.
2 R. Feng, R. Fu, Z. Duan, C. Zhu, X. Ma, D. Fan and X. Li, *J. Biomater. Sci., Polym. Ed.*, 2018, **29**(12), 1463–1481.
3 J. Boateng and O. Catanzano, *J. Pharm. Sci.*, 2015, **104**(11), 3653–3680.
4 A. Kirschning, N. Dibbert and G. Dräger, *Chem. Eur. J.*, 2018, **24**(6), 1231–1240.
5 X. Zhang, D. Yao, W. Zhao, R. Zhang, B. Yu, G. Ma and F. J. Xu, *Adv. Funct. Mater.*, 2021, **31**(8), 2009258.
6 A. Kumari and B. Singh, *Int. J. Biol. Macromol.*, 2024, 130814.
7 F. V. Silva, I. S. Oliveira, K. A. Figueiredo, F. B. Melo Júnior, D. A. Costa, M. H. Chaves and R. C. Oliveira, *J. Med. Food.*, 2014, **17**(6), 694–700.
8 J. A. Sousa, I. S. Oliveira, F. V. Silva, D. A. Costa, M. H. Chaves, F. A. Oliveira and R. C. Oliveira, *J. Biosci.*, 2012, **67**(3–4), 163–171.
9 N. A. Ibrahim, M. H. Abo-Shosha, E. A. Allam and E. M. El-Zairy, *Carbohydr. Polym.*, 2010, **81**(2), 402–408.
10 N. R. Galla and G. R. Dubasi, *Food Hydrocolloids*, 2010, **24**(5), 479–485.
11 H. Bera, Y. F. Abbasi, M. S. Hasnain and A. K. Nayak, In *Natural Polysaccharides in Drug Delivery and Biomedical Application*, 2019, pp. 223–247.
12 E. Drápalová, L. Michlovská, H. Poštulková, I. Chamradová, B. Lipový, J. Holoubek and L. Vojtová, *ACS Appl. Polym. Mater.*, 2023, **5**(4), 2774–2786.
13 V. Raj, J. H. Lee, J. J. Shim and J. Lee, *Carbohydr. Polym.*, 2021, **258**, 117687.
14 S. S. Bahulkar, N. M. Munot and S. S. Surwase, *Carbohydr. Polym.*, 2015, **130**, 183–190.
15 B. K. Preetha and B. Vishalakshi, *J. Environ. Chem. Eng.*, 2020, **8**(2), 103608.
16 N. Prasad, N. Thombare, S. C. Sharma and S. Kumar, *Polym. Bull.*, 2023, **80**(4), 3425–3447.
17 S. J. Kim, H. I. Kim, S. J. Park and S. I. Kim, *Sens. Actuators, A*, 2004, **115**(1), 146–150.
18 J. H. Lee and S. H. Oh, *J. Biomed. Mater. Res.*, 2002, **60**(1), 44–52.
19 S. J. Hong, Y. R. Kwon, S. H. Lim, J. S. Kim, J. Choi, Y. W. Chan and D. H. Kim, *Polym. Plast. Technol.*, 2021, **60**(11), 1166–1175.
20 K. N. Mangang, P. Thakran, J. Halder, K. S. Yadav, G. Ghosh, D. Pradhan and V. K. Rai, *J. Biomater. Sci., Polym. Ed.*, 2023, **34**(7), 986–1017.
21 D. Ji and J. Kim, *ACS Nano*, 2019, **13**(3), 2773–2785.
22 M. Contardi, D. Russo, G. Suarato, J. A. Heredia-Guerrero, L. Ceseracciu, I. Penna and I. S. Bayer, *J. Chem. Eng.*, 2019, **358**, 912–923.
23 O. Z. Higa, S. O. Rogero, L. D. B. Machado, M. B. Mathor and A. B. Lugao, *Radiat. Phys. Chem.*, 1999, **55**(5–6), 705–707.
24 I. A. Alsarra, A. Y. Hamed, G. M. Mahrous, G. M. El Maghraby, A. A. Al-Robayan and F. K. Alanazi, *Drug Dev. Ind. Pharm.*, 2009, **35**(3), 352–362.
25 K. Kuperkar, L. I. Atanase, A. Bahadur, I. C. Crivei and P. Bahadur, *Polymers*, 2024, **16**, 206.
26 R. Poonguzhali, S. K. Basha and V. S. Kumari, *Int. J. Biol. Macromol.*, 2018, **112**, 1300–1309.
27 R. H. Moghaddam, S. Dadfarnia, A. M. H. Shabani, R. Amraei and Z. H. Moghaddam, *Int. J. Biol. Macromol.*, 2020, **154**, 962–973.
28 T. Mehrabi and A. S. Mesgar, *Biointerfaces*, 2022, **212**, 112338.
29 J. Ali, J. B. Lee, S. Gittings, A. Iachelini, J. Bennett, A. Cram and P. Gershkovich, *Eur. J. Pharm. Biopharm.*, 2021, **160**, 125–133.
30 P. L. Ritger and N. A. Peppas, *J. Controlled Release*, 1987, **5**(1), 37–42.
31 S. Sethi, B. S. Kaith, M. Kaur, N. Sharma and S. Khullar, *J. Biomater. Sci., Polym. Ed.*, 2019, **30**(18), 1687–1708.
32 G. Singhvi and M. Singh, *Int. J. Pharm.*, 2011, **2**, 77–84.
33 S. Braune, R. A. Latour, M. Reinthaler, U. Landmesser, A. Lendlein and F. Jung, *Adv. Healthcare Mater.*, 2019, **8**(21), 1900527.
34 N. Thirawong, J. Nunthanid, S. Puttipipatkhachorn and P. Sriamornsak, *Eur. J. Pharm. Biopharm.*, 2007, **67**(1), 132–140.
35 I. G. Munteanu and C. Apetrei, *Int. J. Mol. Sci.*, 2021, **22**(7), 3380.
36 D. Zhang, W. Zhou, B. Wei, X. Wang, R. Tang, J. Nie and J. Wang, *Carbohydr. Polym.*, 2015, **125**, 189–199.
37 L. Luis, G. Alexander, A. Lilian and T. Cristian, *J. Food Eng.*, 2021, **290**, 110230.
38 S. Wittaya-areekul and C. Prahsarn, *Int. J. Pharm.*, 2006, **313**(1–2), 123–128.
39 C. Chen, L. Liu, T. Huang and Q. Wang, *Int. J. Biol. Macromol.*, 2013, **62**, 188–193.
40 K. Y. Lee, J. Shim and H. G. L. Carbo, *Poly.*, 2004, **56**(2), 251–254.
41 K. K. Mali, V. S. Ghorpade, R. J. Dias and S. C. Dhawale, *Int. J. Biol. Macromol.*, 2023, **236**, 123969.
42 O. Sherlock, A. Dolan, R. Athman, A. Power, G. Gethin, S. Cowman and H. Humphreys, *BMC Complementary Altern. Med.*, 2010, **10**, 1–5.
43 S. Bashir, Y. Y. Teo, S. Ramesh and K. Ramesh, *Polymer*, 2018, **147**, 108–120.
44 S. Rehmani, M. Ahmad, M. U. Minhas, H. Anwar, M. I. U. D. Zangi and M. Sohail, *Polym. Bull.*, 2017, **74**, 737–761.
45 M. Venkatesham, D. Ayodhya, A. Madhusudhan, A. Santoshi Kumari, G. Veerabhadram and K. Girija Mangatayaru, *J. Cluster Sci.*, 2014, **25**, 409–422.
46 M. A. Moharram and M. G. Khafagi, *J. Appl. Polym. Sci.*, 2007, **105**(4), 1888–1893.
47 H. N. Öztop, F. Akyildiz and D. Saraydin, *Microsc. Res. Tech.*, 2020, **83**(12), 1487–1498.
48 L. Marvelys, M. Maritza, S. Lilian, L. de Pinto Gladys and H. Julio, *Food Hydrocolloids*, 2006, **20**(6), 908–913.
49 A. C. F. Brito, D. A. Silva, R. C. de Paula and J. P. Feitosa, *Polym. Int.*, 2004, **53**(8), 1025–1032.

50 A. Bozkurt, Ö. Ekinci and W. H. Meyer, *J. Appl. Polym. Sci.*, 2003, **90**(12), 3347–3353.
51 S. Jin, M. Liu, S. Chen and C. Gao, *Eur. Polym. J.*, 2008, **44**(7), 2162–2170.
52 B. Yousuf, S. Wu and Y. Gao, *Food Chem.*, 2021, **345**, 128859.
53 E. Fosso-Kankeu, H. Mittal, F. Waanders, I. O. Ntwampe and S. S. Ray, *Int. J. Environ. Sci. Technol.*, 2016, **13**, 711–724.
54 A. Rasool, S. Ata and A. Islam, *Carbohydr. Polym.*, 2019, **203**, 423–429.
55 R. Jalababu, S. Satya Veni and K. V. N. S. Reddy, *Int. J. Polym. Anal. Charact.*, 2019, **24**(4), 304–312.
56 H. I. Kim, S. J. Park, S. I. Kim, N. G. Kim and S. J. Kim, *Synth. Met.*, 2005, **155**(3), 674–676.
57 R. V. Kulkarni, F. S. Patel, H. M. Nanjappaiah and A. A. Naikawadi, *Int. J. Biol. Macromol.*, 2014, **69**, 514–522.
58 D. Das, R. Das, P. Ghosh, S. Dhara, A. B. Panda and S. Pal, *RSC Adv.*, 2013, **3**(47), 25340–25350.
59 J. R. Forss, *J. Wound Care*, 2022, **31**(3), 236–242.
60 T. Abdelrahman and H. Newton, *Surgery*, 2011, **29**(10), 491–495.
61 A. Higuchi, K. Shirano, M. Harashima, B. O. Yoon, M. Hara, M. Hattori and K. Imamura, *Biomaterials*, 2002, **23**(13), 2659–2666.
62 K. E. Balan, C. Boztepe and A. Künkül, *J. Drug Deliv. Technol.*, 2022, **75**, 103671.
63 F. Prüfert, U. Hering, S. Zaichik, N. M. N. Le and A. Bernkop-Schnürch, *Int. J. Pharm.*, 2020, **583**, 119371.
64 B. Singh and V. Sharma, *Carbohydr. Polym. Technol. Appl.*, 2021, **2**, 100062.
65 S. C. C. C. Silva, E. M. de Araujo Braz, F. A. de Amorim Carvalho, C. A. R. de Sousa Brito, L. M. Brito, H. M. Barreto and D. A. da Silva, *Int. J. Biol. Macromol.*, 2020, **164**, 606–615.
66 I. M. Comino-Sanz, M. D. López-Franco, B. Castro and P. L. Pancorbo-Hidalgo, *J. Clin. Med.*, 2021, **10**(16), 3558.
67 P. G. Rodriguez, F. N. Felix, D. T. Woodley and E. K. Shim, *Dermatol. Surg.*, 2008, **34**(9), 1159–1169.
68 N. Roy, N. Saha, P. Humpolicek and P. Sah, *Soft Mater.*, 2010, **8**(4), 338–357.
69 N. R. Barros, S. Ahadian, P. Tebon, M. V. C. Rudge, A. M. P. Barbosa and R. D. Herculano, *Mater. Sci. Eng. C*, 2021, **119**, 111589.
70 A. Zheng, Y. Xue, D. Wei, S. Li, H. Xiao and Y. Guan, *Soft Mater.*, 2014, **12**(3), 179–187.
71 P. B. Krishnappa and V. Badalamoole, *Int. J. Biol. Macromol.*, 2019, **122**, 997–1007.
72 A. Johnson, F. Kong, S. Miao, H. T. V. Lin, S. Thomas, Y. C. Huang and Z. L. Kong, *Sci. Rep.*, 2020, **10**(1), 18037.
73 A. K. Bajpai and M. Shrivastava, *J. Macromol. Sci., Part A: Pure Appl. Chem.*, 2001, **38**(11), 1123–1139.
74 M. Rahmati and M. Mozafari, *Mater. Today Commun.*, 2018, **17**, 527–540.